Microstructural Characterization of Sn57Bi1Ag Solder Alloy Joints

Sarangapani Murali#, Lim Yee Weon Evonne, Lo Miew Wan, Bayaras Abito Danila, Loke Chee Keong,
Lo Yee Ting, Balasubramanian Senthil Kumar and Kang Sungsig SS,
Heraeus Materials Singapore Pte. Ltd., Ang Mo Kio Ave 5,
TECHplaceII, Blk 5002#04-07, Singapore-569871.
#Corresponding author email address: murali.sarangapani@heraeus.com

Abstract

Sn57Bi1Ag alloy system meets the basic solderability requirements while reliability of solder is less known. The presence of intermetallics that form at the solder-joint interface and in the bulk solder is the primary reason to cause joint failure on simple loading. Furthermore, dissolution of soldered surface (copper, gold, silver, nickel, etc.) into the solder during reflow alters the composition of the interface leading to the formation of intermetallic phases.

The present paper addresses the characterization of low temperature Sn57Bi1Ag solder alloy, its joint interface metallurgy and integrity. Generally, formation of intermetallic phases (Cu_3Sn, Cu_6Sn_5, Ag_3Sn, $AuSn_2$, Ni_3Sn_4, etc.) at the solder-pad interface is in the range of 0.3 to 1.0µm. On thermal ageing at 75°C (0.55Tm), the intermetallic phases grow further up to 2.3µm, particularly CuSn and AuSn phases. In addition, to distributed eutectic tin (Sn) and bismuth (Bi) phases, fine eutectic tin and bismuth phases and primary tin (β-Sn) are also observed. Coarsening of Bi and Sn phases is noticed on thermal ageing (75°C and 100°C). The rate of coarsening increases with the supply of thermal energy promoting Sn/Bi atomic diffusion and movement of eutectic boundaries (grain boundaries). However, the Sn-Bi interface is stable without any significant changes in eutectic structures and its morphologies. The mechanical drop test of the Sn57Bi1Ag solder joint passed 120 drops, characteristic life corresponds to the number of drops for a failure of 63.2%. Evaluated as per JESD22-B111 specification to a maximum peak acceleration of 1500G and half-sine shock pulse duration of 0.5 milliseconds, soldered the alloy to copper OSP surface. The solder joint also passed 1200cycles evaluated at -40 to +125°C. Electrical connectivity of the solder joints soldered to ENIG plated test boards is recorded continuously. Crystallographic orientation of Sn and Bi second phases is observed using electron back scattered diffraction (EBSD) of thermal aged solder joints and are also presented in this paper.

Key words

SnBiAg solder alloy, thermal ageing, mechanical drop test, thermal cycling test

I. Introduction

The performance of solders is important on the functioning of various levels of advanced micro-electronic packaging like flip-chip connection, solder-ball connection in ball-grid-arrays (BGA), or IC package assembly to a printed circuit board (PCB). SAC305 alloy have been commonly used in packaging for a long time, playing a crucial role for metal interconnection in the assembly of modern electronic circuits. The eutectic or near-eutectic SAC alloy has advantages such as ease of handling, good workability, ductility, and excellent wetting with copper and its alloys. It is commonly observed that the solder ball consists of a β-Sn phase with a fine dispersion of Ag_3Sn and Cu_6Sn_5 intermetallic compounds (IMCs) as a second phase. Due to the anisotropic nature of the tetragonal lattice structure of β-Sn, SAC solders are inhomogeneous and isotropic materials, and the mechanical responses of SAC solders are direction-sensitive [1-2]. Thus, the grain structure including grain sizes and orientations is a vital factor influencing mechanical behaviors of SAC solder ball and joint.

In the design of low temperature solder alloys, brittle Sn57Bi1Ag satisfies many of the factor's wettability, solderability, manufacturability, reliability, etc. The solder alloy revealed good wettability with Cu, Ag, Au, Sn, Pd, Ni surfaces. Solderability of the joints strongly depends on the surface morphology to be wetted (oxidation, contamination, roughness) to attain a reliable soldered joint [3-5]. Sn58Bi and Sn57.6Bi0.4Ag solders showed an approximately doubled characteristic lifetime (number of cycles) compared with conventional Sn37Pb solder. Upon microalloying Ag, lifetime of Sn58Bi was marginally increased. Eutectic microstructure of Sn58Bi alloy and Ag_3Sn intermetallic compound were refined. In addition, intermetallic compound

enhances strength through precipitation hardening mechanism of Sn57.6Bi0.4Ag solder, leading to enhanced reliability performance [6]. Sn grain orientation dominated the dissolution of the Ni substrate and the precipitation of IMC inside Sn_3Ag. Ageing at 150°C for 48h coarsen the Sn grain size, altering the orientation of grain, promoting <100> and <110>. Thermo-migration and current crowding played no role. Additionally, it was found that the direction of serrated cathode dissolution exhibited a strong correlation with Sn grain orientation. These effects were explained in terms of the extreme anisotropy of Ni diffusion in Sn [7]. The present findings discuss on the mechanical and electrical properties of Sn57Bi1Ag solder alloy, thermal cycling and drop tests performance of the solder joints, thermal ageing of the solder joints at 75°C and 100°C, correlating with the microstructure of Bi phase distributions. EBSD of solder joints are also discussed.

II. Experiments

Sn57Bi1Ag solder powders were produced using Welco™ processing, melting the alloy slightly to a higher temperature of solder alloy melting point (138°C). Welco™ produced spherical, un-agglomerated particles with clean and smooth surfaces. The oxygen content of T6 powder particles was in the order of few hundred ppm measured using Instrumental Gas Analysis (IGA). Stencil printing revealed good solderability for the reported oxygen level, when maintaining zero printing gap with DEK Horizon 03iX at 25mm/s print speed and 1mm/s squeegee separation speed with 3mm separation distance. Solder paste was thawed for 2h at room temperature before printing, where the temperature ranges from 23 to 27°C and relative humidity (RH) from 50 to 60%. Shear thinning was evident in the initial period of printing say 2h. The paste rolled smoothly, excess hang-up of paste on the squeegee was absent for the tested printing cycles of 8h. Printing solder paste on copper surface for 50µm line spacing and 70µm pad opening revealed absence of bridging.

Mechanical drop test was conducted as per JESD22-B111 specifications to a maximum peak acceleration of 1500G and half-sine shock pulse duration of 0.5 milliseconds. Assembled test board was with 76x76mm PCB, 1.0mm total thickness, 6-layer board, 1/2 oz copper all layers, use IT180A for all layers, 3 mil line with 4 mil space, 4 tooling holes on OSP PCB surface finish. CTBGA208 15x15mm component was soldered to Cu OSP pad surface with Sn57Bi1Ag alloy. Devices were assembled with EP3UF master bond underfill and compared with without underfill samples. Low temperature Sn57Bi1Ag alloy solder was printed to non-solder mask defined (NMSD) with 4mil stencil thickness, 18mils aperture opening, as well targeting 0.33 to 0.5 Bi raise height within the solder sphere. The device was reflowed purging N_2. Characteristic life of Sn57Bi1Ag soldered joints was defined corresponding to number of drops for 63.2% of failure in comparison to SAC305. Thermal cycling was practiced for the profile -40/125°C with 16.5 minutes ramp up and down (10°C per minute) and 15 minutes dwell time at 125°C and 10 minutes dwell time at -40°C. Electrical conductivity of the solder joints has been recorded continuously. ENIG plated test boards were used for thermal cycling studies and Cu OSP substrate were practiced for mechanical drop evaluations.

Main steps adopted in Electron Backscattered Diffraction Pattern (EBSD) analysis of solder ball: sample preparation, finding Kikuchi pattern and component calculation. Solder balls were first potted using epoxy and polished as per standard metallographic technique. Ion milling was applied in the final sample preparation step to remove any mechanical deformation, contamination, and oxidation layer on solder ball surface. The ion-milled sample surface was sputtered with gold. Sample was loaded in a FESEM (field emission scanning electron microscope) with a 70° angled holder to the normal sample holding table surface. The FESEM was equipped with an EBSD detector. The electron back-scattering patterns (EBSP) which contain the crystallographic information were obtained. To distinguish different texture component, maximum tolerance angle of 18-20º was used. Twin boundaries (also called Σ3 CSL twin boundaries) were excluded in the grain size calculation. The twin boundary was described by a 60° rotation about <111> plane of orientation between the neighboring crystallographic domains. The number of observations depended on the step size (40nm), EHT (25kV), scanning area (1500µm^2) and magnification.

III. Results and Discussion

A. Mechanical, Thermal and Electrical Properties of Solder Alloy

Sn57Bi1Ag solder alloy is tensile tested with 4mm diameter rod machined as per ASTM A370-17 standard revealed higher tensile strength than ductile SAC305 solder alloy (Table.1). Though hypo-eutectic range of Bi containing solder alloy (Sn40Bi1Ag) showed marginally better ductility than eutectic Sn57Bi1Ag alloy, melting point is substantially high by 23°C. Thus, higher delta temperature difference between reflow and melting point of the alloy for eutectic composition is an advantage to possess better fluidity, wettability and solderability. The noticeable observation is impact energy of Sn57Bi1Ag alloy is of 0.9J close to glass materials when tested using Charpy-V-notch specimen, machined as per ASTM A370-2019 standard. Young's modulus is measured by ultrasonic testing method as per ASTM C597 standard. Thus, the mechanical behavior of ductile SAC305 is incomparable with Sn57Bi1Ag alloy

brittle in nature. However, low melting point drives the industry to utilize as a potential low temperature solder alloy with good solderability. Typical microstructures of the low temperature Sn57Bi1Ag solder and ductile SAC305 are shown in Figs.1a & b. On tensile pull or Charpy impact, network of Bi second phase leads to cleavage fracture mode, while SAC305 reveal ductile break mode (Figs.1c to f). Measured electrical resistivity of Sn57Bi1Ag using 4 probe testers as per ASTM F84 standard is three and half times higher than SAC305. Hence, it is expected thermal conductivity of Sn57Bi1Ag to be lower than SAC305 due to inferior electron flow in the alloy system (Table.2).

Table.1 Measured mechanical properties of Sn57Bi1Ag and SAC305 solder alloys.

Alloy	Young's Modulus, GPa	Yield/ Tensile Stress, N/mm^2	Ductility, %	Impact Energy, J	Hardness, HV (50mN/5s)
Sn57Bi1Ag	38	63.0/78.0	22.8	0.88	22
Bi phase in Sn matrix					
SAC305	54	35.8/46.6	44.6	69	21
Ag_3Sn network in Sn matrix					

Table.2 Measured electrical and thermal properties of Sn57Bi1Ag and SAC305 solder alloys.

Alloy	Electrical resistivity, μΩ.cm	Thermal conductivity, W/m°K	Temperature, °C		
			Solidus	Liquidus	Reflow
Sn57Bi1Ag	34.9	20.7	139	141	190
SAC305	10.9	64.3	217	223	250

B. Thermal Cycling and Mechanical Drop Tests of Sn57Bi1Ag Solder Joint

Industries are generally looking for thermal cycling and mechanical drop tests of Sn57BiAg solder alloy joint to be adopted in the device assembly. Present reliability studies on low temperature solder (LTS) paste are conducted with the support of external research Institutes. Test boards were assembled using LTS paste formulated with Sn57Bi1Ag solder alloy T6 powder particles. Viscosity of the paste was formulated of about 165 Pa.s. A quick laboratory test on wetting by applying the LTS solder paste on Cu OSP substrate surface revealed good flow (spread) without spalling. The spread of LTS solder at 190°C reflow is as good as SAC305 solder paste flow at 250°C. Interestingly, the brittle Sn57Bi1Ag solder paste passed 120 drops (Table.3)

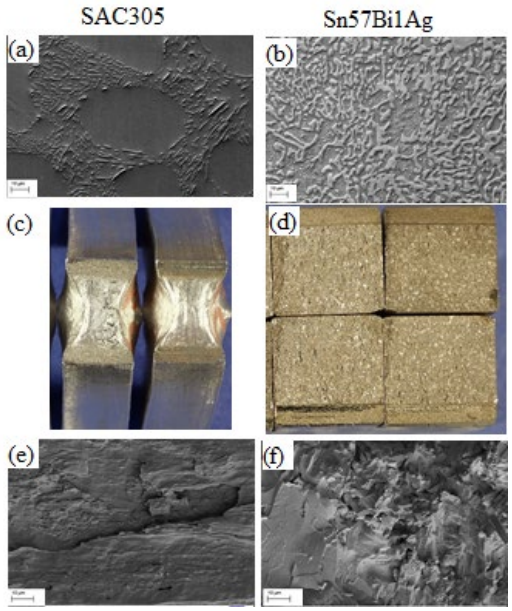

Fig.1 Observations of Sn57Bi1Ag and SAC305 alloys for the conditions; microstructure of cast 4mm rod (a) SAC305 and (b) Sn57Bi1Ag alloy, macro-view of the fractured Charpy-v-notch image, (c) SAC305 and (d) Sn57Bi1Ag alloy, fractography of impacted Charpy sample (e) SAC305 and (f) Sn57Bi1Ag alloy.

for 1500G, 0.5ms pulse curve in comparison to ductile SAC305 solder paste which passed 300drops. Though there are no target values on the number drops to pass, passing 100drops for high acceleration load test is considered as a reliable LTS solder joint. Similarly, thermal cycling of LTS solder alloy joint from -40°C to +125°C temperature demonstrated passing 1200 cycles, behaving nearly the same to that of SAC305 processed on same time. Usually, the thermal cycling temperature recommended to test LTS is 0 to +100C or -15 to +85°C. Present study evaluated with more stringent temperature ranges, yet the LTS solder joint passed 1000 cycles. At +125°C it's expected Bi to dissolve into Sn matrix being close to eutectic temperature. Moreover, at -40°C contraction of the phases (matrix Sn, Bi particles, Cu_3Sn/Cu_6Sn_5 intermetallic layer) can create high stress on cycling. It is evident that crack is running along the Bi particles indicating that the weakest micro-interface to initiate and propagate crack is Sn and Bi interfaces (Fig.2).

Paste	Sn57Bi1Ag		SAC305	
Finish (Au plated)	ENIG		ENIG	
Component	CTBGA208	SMR	CTBGA208	SMR
Number of components	18	36	18	36
Number of failed components until 1500 cycles	1	0	3	1
1st Failure on thermal cycling	1243	-	1175	-
Finish (Cu OSP)	Cu		Cu	
Component	CTBGA		CTBGA	
Number of components	16		16	
Number of failed components until 100 drops	0		0	
1st Failure on mechanical drop	127		314	

Table.3 Thermal cycling and mechanical drop tests of Sn57Bi1Ag and SAC305 solder alloys.

On both drop and thermal cycling tests, basically crack initiate at the interface between Sn57Bi1Ag solder joints and substrate (Fig.2). It is expected that the crack initiation to be slow on thermal cycling, while catastrophic on mechanical drop test. The interface failure on thermal cycling and mechanical drop are inherent behavior of Sn57Bi1Ag solder joint. Closer look of the interface revealed co-existence of Cu_3Sn and Cu_6Sn_5, as well cracks are concentrated in the solder corners indicating crack initiation is perhaps focused on the edges.

C. Mechanical Drop Test of Sn57Bi1Ag Solder Joint with and without Underfill

Resin reinforced low temperature solder paste examined worldwide for the last few years showed benefits in the improvement on the reliability of SnBi solder joint [8]. Similarly, strengthening the interfaces at solder joint corners, arrest crack initiation and lead to improved reliability performance of the solder joint. Present study investigated the benefit of LTS solder joints with underfill. Mechanical drop test at 1500G acceleration is examined for with and without underfill samples. As expected, the benefit of underfill supported solder joint showed 5.5 times longer reliable life compared to solder joint assembled without underfill (Table.4).

Slightly lower reflow temperature (170°C) and shorter time (57s TAL) during assembling of the test boards lead to relatively lower drop test results compared to previous results (Table.3, reflow at 190°C and longer time (158s TAL)). This indicates assembling process optimization is important to attain good solderability of the joint consequently to achieve longer reliability.

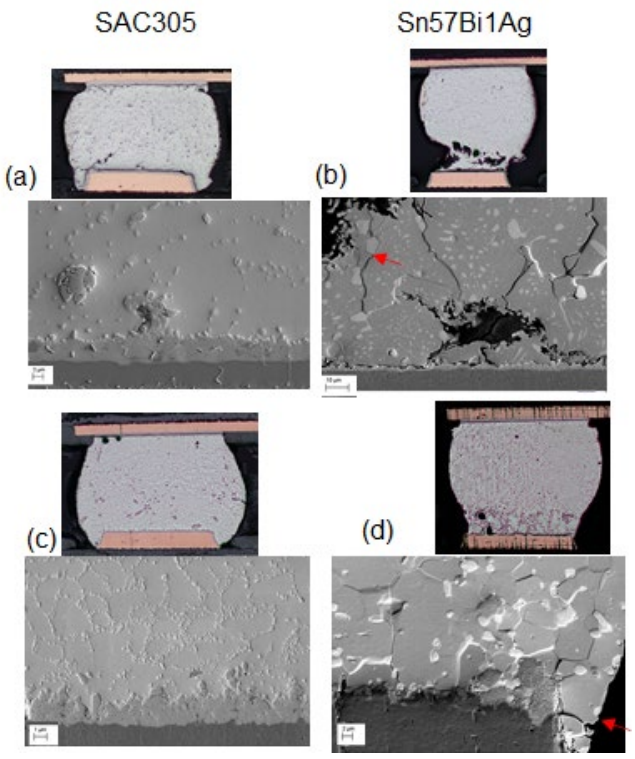

Fig.2 Observations of Sn57Bi1Ag and SAC305 solder joints for the conditions: (a) 1500cycles thermal cycled SAC305 solder joint without interface fracture, (b) 1500cycles thermal cycled Sn57Bi1Ag solder joint with crack running along Bi particles, (c) 130drops tested SAC305 with intact bonding, and (d) 130drops tested Sn57Bi1Ag failed joint.

Paste	With Underfill	Without Underfill
Finish (Cu OSP)	Cu	Cu
Component	CTBGA	CTBGA
Number of components	16	16
1st Failure on mechanical drop	220	40

Table.4 Mechanical drop tests of Sn57Bi1Ag solder joint evaluated with and without underfill.

D. Coarsening (Oswalt Ripening) of Sn57Bi1Ag Solder on Thermal Ageing

A typical microstructure of the Sn57Bi1Ag solder bump reveals distributed Sn-Bi eutectic structure (Fig.3a). Interestingly, fine distributed eutectic structure (Bi phase < 0.5µm long) is observed in between the network of coarser Sn-Bi eutectic phases (Bi phase 2 to 25µm long). Energy dispersive X-ray (EDX) analysis on the Bi phase (white) showed pure 100% bismuth. However, EDX on eutectic tin phase (grey) revealed a solid solution with 5wt% bismuth dissolved into eutectic tin phase. This observation agrees

well with Sn-Bi phase diagram exhibiting β-Sn dissolves up to 5wt% Bi at room temperature. In addition, a few course Ag_3Sn phases are seen in the cross-section of solder bump. Depending on the surface of Sn57Bi1Ag alloy to be soldered, the formation of intermetallic phase types and its thickness differs (Fig.3c). Primarily the intermetallic phases observed at the interface form with tin and none with bismuth. On thermal ageing at 75°C and 100°C the interface intermetallics grow, especially copper-tin phase grows up to 2.4µm for 1000h of storage period (Fig.3c). From SEM-EDX analysis identify Cu_6Sn_5 form and grow to a few microns thickness with Cu OSP surface. Moreover, identify nickel-tin intermetallic phase form co-existing with gold-tin and silver-tin phases when soldered on to ENIG and ENEPIG plated surfaces.

On thermal ageing the solder bumps, the size and morphology of both eutectic tin and bismuth phases grows from fine to coarser (Fig.3b). Surprisingly, tin phase reveals pure tin precipitating the dissolved bismuth. At high magnification, the interface between eutectic tin - bismuth phases are intact without any voids, coalescences of vacancies occurred. The solid-state atomic diffusion and coarsening of the structure on thermal ageing does not create nano or micro voids. The growth of coarser bismuth and tin phases sacrificing finer phases indicates atomic rearrangements occurred by Oswalt ripening mechanism. EDX analysis of certain area (box) clearly revealed high variation in Sn and Bi content ±2wt% at time zero to ±6% after 1000h of ageing at 75°C storage (Fig.3d). Component shear strength of 201 soldered component showed marginal loss of strength after 1000h of storage at 100°C than time zero. However, the shear strength is far above the minimum stress (100g) soldered to copper OSP and gold plated ENIG surfaces. Cross-sectioning close to fractured solder joint interface, clearly showed crack running along Bi particles, between tin and bismuth interface (Figs.2b & d).

E. EBSD Analysis of Sn57Bi1Ag Solder Joint and on Thermal Ageing

Grain size and crystallographic orientation of the solidified solder ball revealed low fraction of higher symmetry texture components (<100>, <110>) and an average grain size of ~3µm on Sn-Bi solder paste. In addition, grains revealed wide range of fraction of <111>, <113> and <210> plane of orientations (Table.5). Thermal aged solder joints and bumps at 100°C for 375/1000h revealed closer fraction of plane of orientations corresponding to β-Sn regions. EBSD is recorded for mis-orientation angle of 10° and 18°. Though grains and eutectic bismuth particles morphology have significantly altered, no predominant change in plane of orientations are evident (Fig.4 and Table.5).

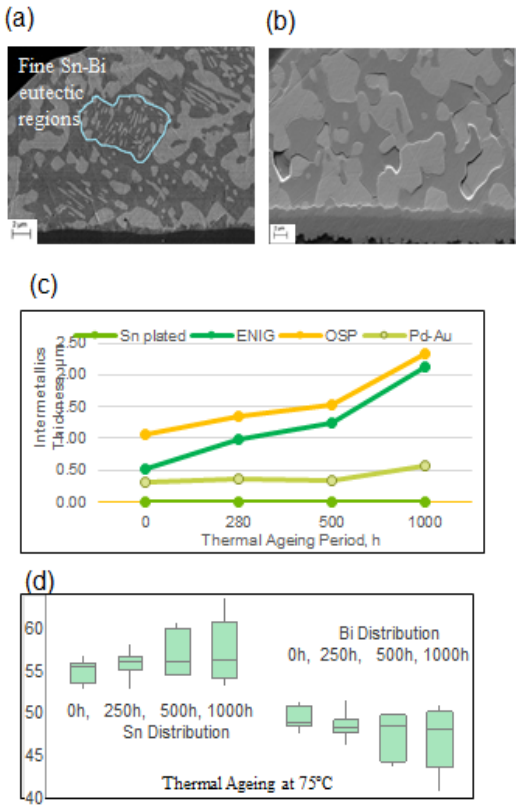

Fig.3 Observations of Sn57Bi1Ag solder alloy for the conditions: (a) cast (reflow) microstructure, (b) thermal aged microstructure (c) growth of intermetallics at Sn57Bi1Ag interface soldered to different plated surfaces and (d) Weight percentage (wt.%) distribution of Sn and Bi phases of the solder bumps on EDX.

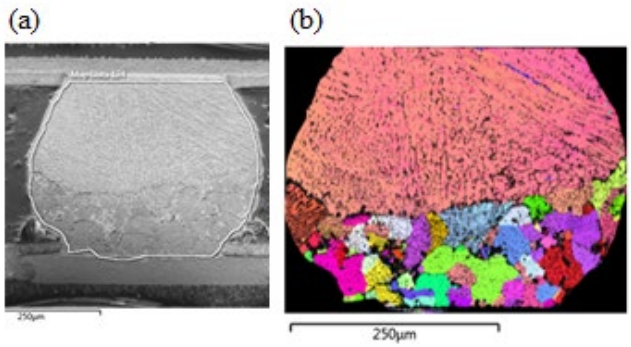

Fig.4 Observations of Sn57Bi1Ag solder joint alloy for the conditions: (a) microstructure of thermal aged at 100°C for 375h and (b) inverse pole figure (IPF) image of the solder joint (SAC sphere soldered with Sn57Bi1Ag alloy).

% Texture component				
Thermal Ageing at 100°C, 375h				
<100>	<110>	<111>	<113>	<210>
0.05 – 5.71	0.10 -15.00	0.33 – 42.40	2.89 – 73.80	0.09 – 33.60
Time zero				
<100>	<110>	<111>	<113>	<210>
0.28 - 13.0	0.63 - 12.7	1.01 - 45.1	19.7 - 68.5	3.27 - 16.4

Table.5a EBSD analysis of Sn57Bi1Ag solder joint thermal aged at 100°C for 375h.

% Texture component				
Thermal Ageing at 100°C, 1000h				
<100>	<110>	<111>	<113>	<210>
1.12 – 17.0	1.04 - 22.0	1.88 - 29.8	2.19 - 35.9	2.83 - 32.3
Time zero				
<100>	<110>	<111>	<113>	<210>
0.02 – 1.65	0.04 - 5.86	0.04 - 33.1	19.2 – 51.5	0.39 - 6.61

Table.5b EBSD analysis of Sn57Bi1Ag solder bump thermal aged at 100°C for 1000h.

III. Conclusion

Low temperature Sn57Bi1Ag solder joint reveal brittle behavior compared to ductile SAC305. Mechanical drop and thermal cycling tests revealed reliable performance of LTS Sn57Bi1Ag solder joint passed 120drops and 1200cycles, respectively. Mechanical drop test of LTS solder joint with underfill showed 5.5 times better in reliability performance than without underfill solder joint. On thermal ageing, obvious coarsening of Bi and Sn phases is observed. However, no degradation in component shear strength is observed at 75°C ageing (0.55Tm) up to 1000 hours with stable interface. Whereas thermal Ageing at 100°C (0.72Tm) revealed slight degradation in shear strength. Significant growth of copper-tin phase is noticed when LTS soldered with copper surface and aged up to 1000h. EBSD analysis of the solder ball exhibited <111>, <113> and <210> texture components of β-Sn grains. On thermal ageing at 100°C, though grain size remained unchanged, size and morphology of Bi particles and eutectic Sn phases have been significantly altered.

Acknowledgments

Authors are grateful to Mr. Joanne Chong and Ms. Sylvia Sutiono, Mr. Yam Lip Huei for their experimental support.

References

[1] Jing Zou, "Effects of Grain Size and Orientation on Mechanical Response of Lead Free Solders", *Master of Science Thesis*, Auburn University, Alabama, 13 December 2013.

[2] N. Zhao, Y. Zhong, W. Dong, M. L. Huang, H. T. Ma, and C. P. Wong, "Formation of highly preferred orientation of β-Sn grains in solidified Cu/SnAgCu/Cu micro interconnects under temperature gradient effect", *Applied Physics Letters,* 110, 093504 1-5, 2017.

[3] K. Dušek, D. Bušek, P. Veselý, A. Pražanová, M. Plaˇcek and J. Del Re, "Understanding the Effect of Reflow Profile on the Metallurgical Properties of Tin–Bismuth Solders", *Metals*, 12, 121, 2022.

[4] Y. Maruyaa, H. Hataa, I. Shohjia, S. Koyamaa, "Bonding Characteristics of Sn-57Bi-1Ag Low-Temperature Lead-Free Solder to Gold-Plated Copper", *Procedia Engineering*, 184, 2017, pp 223-230.

[5] S. Murali, L. Y. W. Evonne, A. Joel, L. Y. Ting, L. H. Yam, L. M. Wan, L. C. Keong, B. Senthilkumar, F. Sebastian, SS Kang, C. L. San and Z. HanWen, "A Study on Interfacial Intermetallic Phases at Sn-Bi Solder Joint", *LTS2021, Virtual conference on low temperature solder*, 16th June, 2021.

[6] G. Ren and M. N. Collins, "Improved Reliability and Mechanical Performance of Ag Micro-alloyed Sn58Bi Solder Alloys", *Metals*, 9, 462, 2019, pp 1-10.

[7] T.C. Huang, T.L. Yang, J.H. Ke, C.H. Hsueh and C.R. Kao, "Effects of Sn grain orientation on substrate dissolution and intermetallic precipitation in solder joints under electron current stressing", *Scripta Materialia*, 80, 2014, pp 37-40.

[8] Haley Fu, R. Jagadeesh, R. Morgana, A. Raiyo, A. Babak, B. Kevin Byrd, C. Antonio, C. Jimmy, C. Qin, C. Richard, D. Derek, F. Sophia Feng, G. Pubudu, L. Ralph, M. Francis, S. Murali, T.K. Kwan, T. Kris, W. Daniel, W. Greg, Z. Hongwen, Z. Wilson, "iNEMI project on process development of BiSn based low temperature solder pastes, Part VI, mechanical shock results on resin reinforced mixed SnAgCu-BiSn solder joints of FCBGA components", *Proceedings of SMTA International*, Rosemont, IL, USA, Sept. 22-26, 2019.